Excitation functions of coupling

Tianshou Zhou*
School of Mathematics and Computational Science, Zhongshan University, Guangzhou 510275, People's Republic of China

Luonan Chen† and Ruiqi Wang
Department of Electrical Engineering and Electronics, Osaka Sangyo University, Daito, Osaka 574-8530, Japan
(Received 7 May 2004; revised manuscript received 29 July 2004; published 22 June 2005)

The responses of nonlinear dynamics of two classes to coupling are investigated. It is shown both analytically and numerically that coupling has an excitation ability in a network of the linearly coupled systems. That is, when an uncoupled system is degenerated to a stable steady state from a limit cycle but in the "marginal" state due to the system parameter, an appropriate coupling strength can excite the limit cycle such that the coupled systems exhibit synchronous oscillation; when the uncoupled system is in a stable limit cycle but close to a chaotic attractor, a certain coupling strength can induce the chaotic attractor such that the coupled systems reach chaotic synchronization. Such excitation functions of coupling are different from its traditional role where coupling mainly synchronizes the coupled systems with the original dynamics of the uncoupled system.

DOI: 10.1103/PhysRevE.71.066211 PACS number(s): 05.45.Xt, 05.70.Fh

I. INTRODUCTION

In the recent decades, collective phenomena in nonlinear science have attracted extensive attention with discovery of different types of oscillatory behaviors, such as chaotic synchronization [1–4] and stochastic resonance or coherence resonance [5–11]. There are many examples demonstrating that the collective behavior of systems composed of interacting functional units can be regulated by a cooperative mechanism, e.g., synchronization.

Synchronization phenomena exist in many biologically plausible models [12–23]. Recent studies show that the intercellular communication is accomplished by synchronization [10,17,24–28], and a number of simulations and fundamental experiment works also confirm the synchronization mechanism in some biological systems [29,30]. Such communication and synchronization may facilitate fundamental biological functions. For example, it is possible that coupling can act as a stimulus to induce a cell to fire in a case where, without coupling, it would be unable to produce an action potential. Studying this problem is of great significance from the biological viewpoint, which motivates the study of this paper.

Another motivation is from the theoretical aspect of dynamics. Although type, mode, and strength of coupling are crucial to the dynamics of coupled systems, the traditional function of coupling is to mainly synchronize the coupled systems with the original dynamics of the uncoupled systems. For example, when an uncoupled system is an oscillator, an appropriate coupling strength can drive these identical oscillators to be synchronized [31]; when the uncoupled system has a chaotic attractor, a certain coupling strength can force the linearly coupled identical systems to accomplish chaotic synchronization [32]. In both cases, the fundamental dynamics of the two kinds of coupled systems remains unaltered by the synchronization. However, besides such a simple synchronization function, coupling may have other effects on interacting systems.

This paper reports that coupling has an excitation ability to excite or recover some potential dynamics of uncoupled systems. We consider an interconnected system of identical subsystems without external driving force, and the corresponding coupling is all-to-all and bidirectional. We find that when the uncoupled system loses its stable limit cycle and is in a stable steady state due to the system parameter, an appropriate coupling strength can excite the limit cycle such that coupled systems have a synchronous oscillation. When the individual subsystems are near a chaotic parameter regime, the excitation function of coupling is also conspicuous, e.g., when a stable limit cycle is in the marginal state to a chaotic attractor in the uncoupled system, a certain coupling strength can push the coupled systems into chaotic synchronization. These two cases imply that coupling acts as a compensating energy to "lift" dynamical behaviors of the uncoupled system from a stable fixed point to a limit cycle and from a limit cycle to a chaotic attractor, and at the same time pushes the coupled systems into synchronization.

II. LIMIT CYCLE CASE

Suppose a network composed of N identical cells is coupled in an all-to-all way (see Fig. 1). Each cell may be regarded as a chemical system with m distinct chemical species, and is assumed to obey kinetic equations in the vector form

$$\frac{dZ}{dt} = f(Z), \tag{1}$$

where $Z \in \mathbf{R^m}$, representing concentrations of the species. The coupling among the cells is assumed to be linear. The network is mathematically expressed as

*Email address: tszhou@msn.com
†Email address: chen@elec.osaka-sandai.ac.jp

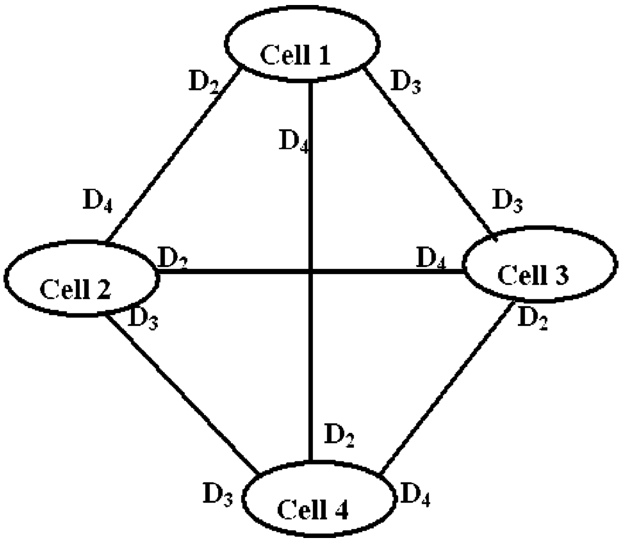

FIG. 1. A schematical sketch of an interconnected network for $N=4$, where the $\mathcal{D}_j$'s neighboring the jth cell represent coupling coefficient matrices of the cell with other cells, e.g., cell 1 is coupled with cell 2 through coupling coefficient matrix $\mathcal{D}_2$ while cell 2 is coupled with cell 1 through the matrix $\mathcal{D}_4$.

$$\frac{dX}{dt} = \mathcal{F}(X) + \mathcal{D}X, \tag{2}$$

where

$$\mathcal{D} = \begin{pmatrix} \mathcal{D}_1 & \mathcal{D}_2 & \mathcal{D}_3 & \cdots & \mathcal{D}_N \\ \mathcal{D}_N & \mathcal{D}_1 & \mathcal{D}_2 & \cdots & \mathcal{D}_{N-1} \\ \vdots & \vdots & \vdots & & \vdots \\ \mathcal{D}_2 & \mathcal{D}_3 & \mathcal{D}_4 & \cdots & \mathcal{D}_1 \end{pmatrix}, \quad \mathcal{F}(X) = \begin{pmatrix} f(X_1) \\ f(X_2) \\ \vdots \\ f(X_N) \end{pmatrix}$$

with $D_j \in \mathbf{R}^{\mathbf{m}\times\mathbf{m}}$ $(1 \leqslant j \leqslant N)$.

Note that when the couplings satisfy the conservation condition (the condition is always assumed throughout the paper),

$$\sum_{i=1}^{N} \mathcal{D}_i = \mathcal{O}\ (\text{zero matrix}), \tag{3}$$

Eq. (2) may be rewritten as the following standard coupling form:

$$\frac{dX_1}{dt} = f(X_1) + \sum_{j=1}^{N} \mathcal{D}_j X_j = f(X_1) + \sum_{j=1}^{N} \mathcal{D}_j (X_j - X_1),$$

$$\begin{aligned} \frac{dX_k}{dt} &= f(X_k) + \sum_{j=1}^{k-1} \mathcal{D}_{N-k+1+j} X_j + \sum_{j=k}^{N} \mathcal{D}_{j-k+1} X_j \\ &= f(X_k) + \sum_{j=1}^{k-1} \mathcal{D}_{N-k+1+j}(X_j - X_k) + \sum_{j=k}^{N} \mathcal{D}_{j-k+1}(X_j - X_k), \end{aligned} \tag{4}$$

where $2 \leqslant k \leqslant N$. Clearly, systems (2) and (4) have all-to-all and bidirectional coupling. In addition, we point out that such a coupling matrix $\mathcal{D}$ with the specific form, i.e., $\mathcal{D}$ is a circular block matrix [33], is only for convenience of the theoretical analysis. In fact, phenomena shown in the paper can take place in coupled nonlinear dynamical systems with different modes of couplings.

We first show that there is a close relation between Jacobian matrices of uncoupled system (1) and coupled systems (2). To do this, we denote by $\mathcal{A}$ and $\mathcal{B}$ the Jacobian matrices of Eqs. (1) and (2) evaluated at their steady states, respectively. According to Appendix A, we have

$$\mathcal{P}^{-1}\mathcal{B}\mathcal{P} = \text{diag}\big(d(\omega_1 I), d(\omega_2 I), \ldots, d(\omega_N I)\big), \tag{5}$$

where $d(x) = \mathcal{A} + \sum_{j=1}^{N} \mathcal{D}_j x^{j-1}$, I is the unit matrix of order m, and ω_j $(1 \leqslant j \leqslant N)$ are N unit roots of the algebraical equation $\omega^N - 1 = 0$ with $\omega_1 = 1$. Since $d(\omega_1) = d(1) = \mathcal{A}$, the matrix $\mathcal{B}$ can be similar to a real block matrix, that is, as shown in Appendix A, there exists a reversible real matrix $\mathcal{Q}$ such that

$$\mathcal{Q}^{-1}\mathcal{B}\mathcal{Q} = \begin{pmatrix} \mathcal{A} & \mathcal{O} \\ \mathcal{O} & \mathcal{R} \end{pmatrix}, \tag{6}$$

where $\mathcal{R}$ is a certain real matrix. The relation between Jacobian matrices of the uncoupled system and the coupled systems implies that the linearization equation of the coupled systems at the steady state can be decomposed into two independent subsystems, one of which is nothing but the linearization equation of the uncoupled systems in its steady state.

By the decomposition, it is reasonable to expect that the coupled systems have an (even stable) limit cycle even though the uncoupled system is still in a stable steady state. To be specific, denote by $\lambda_{\mathcal{B}}$ a characteristic value of the matrix $\mathcal{B}$. Then,

$$\det\left(\lambda_{\mathcal{B}} I - \mathcal{A} - \sum_{j=1}^{N} \mathcal{D}_j e^{[2\pi i(k-1)/N](j-1)}\right) = 0 \tag{7}$$

for $2 \leqslant k \leqslant N$, where $i = \sqrt{-1}$. From Eq. (7), one can obtain all characteristic values of $\mathcal{B}$ including complex ones. To specify these characteristic values, we return to Eq. (6). According to Appendix A, we have for $N = 2K+1$

$$\mathcal{R} = \text{diag}\left(\begin{pmatrix} \mathcal{D}_R(\vartheta_1) & -\mathcal{D}_I(\vartheta_1) \\ \mathcal{D}_I(\vartheta_1) & \mathcal{D}_R(\vartheta_1) \end{pmatrix}, \ldots, \begin{pmatrix} \mathcal{D}_R(\vartheta_K) & -\mathcal{D}_I(\vartheta_K) \\ \mathcal{D}_I(\vartheta_K) & \mathcal{D}_R(\vartheta_K) \end{pmatrix}\right), \tag{8}$$

with $\vartheta_j = 2\pi j/N$ and $1 \leqslant j \leqslant K$; and for $N = 2K$

$$\mathcal{R} = \mathrm{diag}\left(\mathcal{D}_R(\pi), \begin{pmatrix} \mathcal{D}_R(\vartheta_1) & -\mathcal{D}_I(\vartheta_1) \\ \mathcal{D}_I(\vartheta_1) & \mathcal{D}_R(\vartheta_1) \end{pmatrix}, \ldots, \begin{pmatrix} \mathcal{D}_R(\vartheta_{K-1}) & -\mathcal{D}_I(\vartheta_{K-1}) \\ \mathcal{D}_I(\vartheta_{K-1}) & \mathcal{D}_R(\vartheta_{K-1}) \end{pmatrix}\right), \tag{9}$$

with $\vartheta_j = 2\pi j/N$ and $1 \leqslant j \leqslant K-1$, where

$$\mathcal{D}_R(\vartheta) = \mathcal{D}_1 + \mathcal{A} + \mathcal{D}_2 \cos\vartheta + \mathcal{D}_3 \cos 2\vartheta + \cdots + \mathcal{D}_N \cos(N-1)\vartheta,$$

$$\mathcal{D}_I(\vartheta) = \mathcal{D}_2 \sin\vartheta + \mathcal{D}_3 \sin 2\vartheta + \cdots + \mathcal{D}_N \sin(N-1)\vartheta. \tag{10}$$

Observing $\mathcal{R}$ in both cases, one needs to investigate roots of the following characteristic polynomial:

$$p(\lambda) \equiv \left| \lambda I - \begin{pmatrix} \mathcal{D}_R(\vartheta_j) & -\mathcal{D}_I(\vartheta_j) \\ \mathcal{D}_I(\vartheta_j) & \mathcal{D}_R(\vartheta_j) \end{pmatrix} \right|, \tag{11}$$

where $1 \leqslant j \leqslant [(N-1)/2]$. For the case of $N=2K$, one also investigates roots of

$$\left| \lambda I - \mathcal{A} - \sum_{j=1}^{N} (-1)^j \mathcal{D}_j \right| = 0. \tag{12}$$

Note that

$$p(\lambda) = |\lambda I - \mathcal{D}_R(\vartheta_j) - i\mathcal{D}_I(\vartheta_j)||\lambda I - \mathcal{D}_R(\vartheta_j) + i\mathcal{D}_I(\vartheta_j)|. \tag{13}$$

For simplicity, we consider the case of $\mathcal{D}_k \equiv \mathcal{D}_0$ $(2 \leqslant k \leqslant N)$. In this case, we have $\mathcal{D}_R(\vartheta_j) = \mathcal{A} - (N-1)\mathcal{D}_0 + \mathcal{D}_0 \Sigma_{k=1}^{N-1} \cos k\vartheta_j$ and $\mathcal{D}_I(\vartheta_j) = \mathcal{D}_0 \Sigma_{k=1}^{N-1} \sin k\vartheta_j$. Note that

$$\sum_{k=1}^{N-1} \cos k\vartheta_j + i \sum_{k=1}^{N-1} \sin k\vartheta_j = \sum_{k=1}^{N-1} e^{ik\vartheta_j} = -1$$

for $\vartheta_j = 2\pi j/N$ with $1 \leqslant j \leqslant [(N-1)/2]$. Therefore

$$p(\lambda) \equiv |\lambda I - \mathcal{A} + N\mathcal{D}_0|^2 = 0. \tag{14}$$

Also note that Eq. (12) may be included in Eq. (14). Equation (14) has more advantages than Eq. (7) in determining eigenvalues of the matrix $\mathcal{B}$.

On the other hand, assume that the uncoupled system has the potential of a limit cycle or is degenerated to its stable steady state from a limit cycle bifurcated from a Hopf bifurcation point, due to the system parameter. In this case, one needs only to choose such coupling strengths that for some j $(2 \leqslant j \leqslant N)$, a certain $\lambda_{\mathcal{B}}$ satisfying Eq. (14) goes through the imaginary axis. In other words, the coupled systems undergo a Hopf bifurcation. Furthermore, if some $\mathcal{D}_j$ is taken as a bifurcation parameter, then the transversal condition holds since $v_L \mathcal{B}'(\mathcal{D}_j) v_R = (d/d\mathcal{D}_j)\mathrm{Tr}\mathcal{B}(\mathcal{D}_j) = 1$, where v_L and v_R are respectively the left and right characteristic vectors of $\mathcal{B}$ corresponding to characteristic value $\lambda_{\mathcal{B}}$. Thus the coupled systems will have a periodic orbit produced through a Hopf bifurcation. In this sense, we say that the original limit cycle in the uncoupled system is excited or recovered due to effect of the coupling.

Moreover, when a potential limit cycle in the uncoupled system is excited, the corresponding periodic orbit in the coupled systems is practically a synchronization oscillation of all these uncoupled systems, i.e., the coupled systems have an in-phase solution. However, the synchronization is different from the one in the traditional coupled systems since for the latter, the uncoupled system is first assumed to be an oscillator and an appropriate coupling strength then pushes these oscillators to be synchronized. Furthermore, we point out that the procedure of the above analysis in fact implies that we have checked all algebraical conditions in the so-called "global Hopf bifurcation theorem" [34,35]. Therefore such an excited limit cycle is in nature produced through the so-called "global Hopf bifurcation." In addition, theoretically, the coupled systems with the above-specified coupling may have an out-of-phase solution when the strength of the coupling is appropriate, and the out-of-phase solution may be also produced through the global Hopf bifurcation. Generally, the out-of-phase solution through such a mechanism is unstable. Another of our papers [36] discusses the stability of different types of synchronous solutions including in-phase and out-of-phase solutions in detail and derives some sufficient conditions for their stability. Similarly, some sufficient conditions guaranteeing the stability of the excited limit cycle can be derived. Under these conditions, the excited limit cycle is stable, so it is independent of the initial condition. In this case, the corresponding in-phase solution is different from the phase-locking solution in weakly heterogeneous neural networks discussed in Ref. [37]. In that paper, an in-phase solution coexists with an out-of-phase solution, and both can be stable for the suitable coupling strength, so either the stable in-phase solution or the stable out-of-phase solution greatly depends on initial conditions.

Now, we apply the above analytic result to a specific example. For simplicity, consider the Brusselator which is a model of the autocatalytic chemical reaction (see Ref. [38]), and is mathematically described as

$$\begin{cases} \dfrac{dx_1}{dt} = a - (\mu+1)x_1 + x_1^2 x_2 \\ \dfrac{dx_2}{dt} = \mu x_1 - x_1^2 x_2, \end{cases} \tag{15}$$

where $a>0$ and $\mu>0$ are parameters. Equation (15) has the unique steady state $E=(a, \mu/a)$. In addition, introduce a linearly coupled system of two identical Brusselators:

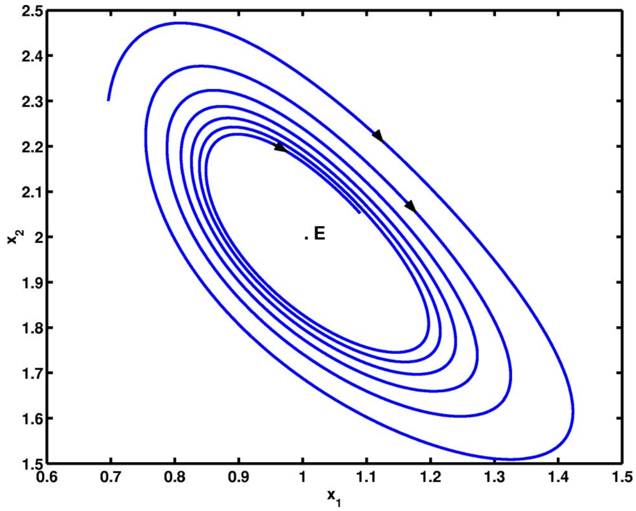

FIG. 2. The steady state $E=(1.0,2.0)$ of the uncoupled Brusselator (15) is stable with parameter values $a=1.0$ and $\mu=2.0$. Arrows in the figure represent the time-evolutionary direction of phase trajectories. Here we only plot one part of the phase trajectories (i.e., the part corresponds to the case that time t is finite). When time t tends to infinity, the trajectories will tend to the steady state.

$$\begin{cases} \dfrac{dx_1}{dt} = a - (\mu+1)x_1 + x_1^2 x_2 + d_1(x_3 - x_1) \\ \dfrac{dx_2}{dt} = \mu x_1 - x_1^2 x_2 + d_2(x_4 - x_2) \\ \dfrac{dx_3}{dt} = a - (\mu+1)x_3 + x_3^2 x_4 + d_1(x_1 - x_3) \\ \dfrac{dx_4}{dt} = \mu x_3 - x_3^2 x_4 + d_2(x_2 - x_4). \end{cases} \tag{16}$$

Using notations of Eq. (2), we have

$$\mathcal{D}_2 = \begin{pmatrix} d_1 & 0 \\ 0 & d_2 \end{pmatrix}$$

and $\mathcal{D}_1 = -\mathcal{D}_2$, where $d_1 > 0$ and $d_2 > 0$ are constants. It is known that for $\mu > a^2+1$, the uncoupled Brusselator has a unique limit cycle [39] whereas for $(a-1)^2 < \mu \leqslant a^2+1$, all its trajectories tend to the steady state. Moreover, the Jacobian matrix evaluated at the steady state has a pair of conjugated complex roots.

As shown in Appendix B, a sufficient condition ensuring that the coupled Brusselators (16) have a stable limit cycle is

$$2(\mu - 2d_1 - 1)d_2 > a^2(2d_1+1). \tag{17}$$

In fact, this condition is also derived from the Hopf bifurcation for the coupled Brusselators. It follows from Eq. (17) combined with $\mu \leqslant a^2+1$ that

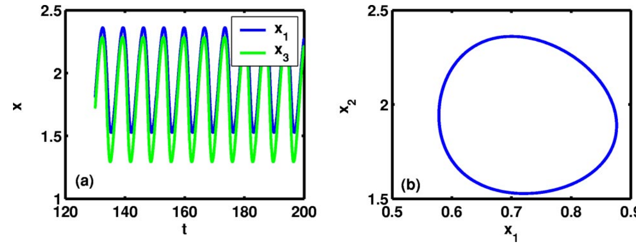

FIG. 3. Synchronous oscillation in the coupled Brusselators (16) with parameter values $a=1.0$, $\mu=2.0$, $d_1=0.2$, and $d_2=3.0$. (a) Time evolution of components x_1 and x_3 in Eq. (16); (b) phase diagram of projection of the corresponding synchronous solution. The initial values are $(x_1,x_2,x_3,x_4)=(-1.5,1.8,1.5,-2.5)$.

$$\text{if } d_1 < \frac{a^2}{2}, \text{ then } d_2 > \frac{a^2(2d_1+1)}{2(a^2-2d_1)} \quad \text{and}$$

$$2d_1 + 1 + \frac{a^2(2d_1+1)}{2d_2} < \mu \leqslant a^2+1. \tag{18}$$

These conditions explicitly show that the coupled Brusselators still have a stable limit cycle even though the uncoupled Brusselator is currently in the stable steady state.

Next, we further verify this result by numerical simulation. Take $a=1.0$ and $\mu=2.0$. In this case, the uncoupled Brusselator has a stable equilibrium (see Fig. 2) whereas its linearly coupled systems with coupling coefficients $d_1=0.2$ and $d_2=3.0$ have a synchronous oscillation, as shown in Fig. 3. This phenomenon indicates that the coupling has excited the original potential limit cycle in the uncoupled Brusselator and pushed the coupled Brusselators to be synchronized.

The numerical simulation also has verified that similar phenomena can occur where $49/30 < \mu \leqslant 2.0$ at fixed $a=1.0$, $d_1=0.2$, and $d_2=3.0$.

We here emphasize that coupling has such an excitation capability only when the uncoupled system has the potential to oscillate or is in the "marginal" state to a limit cycle. Otherwise, coupling cannot induce the synchronization oscillation. For example, when $a=1.0$ and $\mu=0.9$, the uncoupled Brusselator has a stable equilibrium. In this case, however, the coupled Brusselators have no limit cycle whatever d_1 and

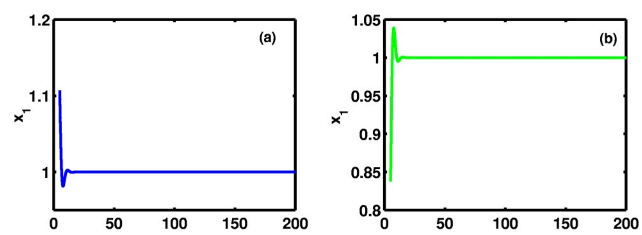

FIG. 4. An example showing that coupling has no excitation capability, where parameters are $a=1.0$ and $\mu=0.9$, and coupling coefficients are $d_1=5.2$ and $d_2=13.0$. In this case, the uncoupled Brusselator is not in "marginal" state to the limit cycle, the coupling cannot excite the original potential limit cycle in the uncoupled Brusselator. (a) Time evolution of x_1 of the uncoupled Brusselator (15); (b) Time evolution of x_1 of the coupled Brusselators (16). In either case, all trajectories tend to a fixed point.

d_2 are, as shown in Fig. 4, because $\mu=0.9$ does not satisfy the necessary condition (i.e., $\mu>1.0$) according to Eq. (18).

Although the above example has dynamical terms of a specific form and a specific coupling, the excitation function of coupling can be found in a wide variety of coupled nonlinear systems. In fact, we also have investigated other examples, such as the coupled Van der Pol oscillators. The key point is that coupling can excite or recover a potential limit cycle of the uncoupled system such that the coupled systems reach phase synchronization.

III. CHAOTIC ATTRACTOR CASE

In the case of chaotic attractors, we can also obtain similar effect of coupling by estimating Lyapunov exponents of uncoupled and coupled systems, respectively. We show below that coupled systems have one positive Lyapunov exponent due to coupling coefficients even though all Lyapunov exponents of the uncoupled system are currently zero or negative.

Generally, Lyapunov exponents of a chaotic system cannot be expressed in an explicit formula. To obtain information on Lyapunov exponents, we here give an approximate scheme according to characteristic of our coupled systems (2). Given an initial state z_0 of the coupled systems, we can have an iterative system:

$$z_{k+1} = \mathcal{G}_k(z_0, z_1, \ldots, z_k). \tag{19}$$

Let $J_k(z)$ be the Jacobian matrix of Eq. (19) evaluated at z in the kth step. Define

$$T_k(z_0) := J_k(z_k)J_{k-1}(z_{k-1})\cdots J_1(z_1)J_0(z_0). \tag{20}$$

Furthermore, let $|\mu_j(T_k(z_0))|$ be module of the jth eigenvalue of the kth matrix $T_k(z_0)$, where $j=1,2,\ldots,mN$ and $k=0,1,\ldots$. By Ref. [40], the jth Lyapunov exponent may be expressed as

$$\lambda_j(z_0) = \lim_{k\to\infty}\frac{1}{k}\ln\{\mu_j(J_k(z_k)\cdots J_1(z_1)J_0(z_0))\}. \tag{21}$$

Note that each $J_k(z_k)$ can be decomposed into one form like Eq. (6), and that all eigenvalues of the corresponding $\mathcal{R}$ satisfy an equation like Eq. (7). Therefore one can reasonably expect that the coupled systems (2) have one positive Lyapunov exponent if the coupling coefficients are appropriately chosen, even though all Lyapunov exponents of the uncoupled system still are zero or negative. For clarity, we consider a simple iteration form for Eq. (2) (in the practical numerical calculation, we take the order-4 Runge-Kutta method):

$$z_{k+1} = (\mathcal{I} + \delta t\mathcal{D})z_k + \mathcal{F}(z_k)\delta t, \tag{22}$$

where $k=0,1,2,\ldots$, δt is step interval, and $\mathcal{I}$ is the unit matrix of order mN. Then $J_k=\mathcal{I}+\delta t\mathcal{D}+\delta t\mathcal{W}_k$, where $\mathcal{W}_k=\mathrm{diag}(\mathcal{A}_1,\mathcal{A}_2,\ldots,\mathcal{A}_N)$ and $\mathcal{A}_k=\partial f(z_k)/\partial\xi$. According to our analysis in the previous section, we have

$$\mathcal{P}^{-1}J_k\mathcal{P} = \mathrm{diag}(g(\omega_1 I), g(\omega_2 I), \ldots, g(\omega_N I)),$$

where $g(x)\equiv\delta t\mathcal{A}_k+I+\delta t\Sigma_{j=1}^{N}\mathcal{D}_j x^{j-1}$, and the matrix $\mathcal{P}$ is given in Appendix A. In particular, the matrix $\mathcal{P}$ is independent of $\mathcal{A}_k$ and $\mathcal{D}_j$ for all k and j. In order to obtain more information about Lyapunov exponents, now we consider a special case: $\mathcal{D}_j\equiv\mathcal{D}_0$ $(2\leqslant j\leqslant N)$. Then, the conservation condition for coupling yields $\mathcal{D}_1=-(N-1)\mathcal{D}_0$. It is easy to verify that $g(\omega_j I)=I+\delta t(\mathcal{A}_k-N\mathcal{D}_0)$ for all $j\in\{1,2,\ldots,N\}$. Note that

$$\begin{aligned}\mathcal{P}^{-1}T_k\mathcal{P} &\equiv \mathcal{P}^{-1}J_kJ_{k-1}\cdots J_1J_0\mathcal{P}\\ &= \mathcal{P}^{-1}J_k\mathcal{P}\cdot\mathcal{P}^{-1}J_{k-1}\mathcal{P}\cdots\mathcal{P}^{-1}J_1\mathcal{P}\cdot\mathcal{P}^{-1}J_0\mathcal{P}.\end{aligned}$$

Therefore we introduce a matrix

$$S_k = \prod_{l=0}^{k}[I + \delta t(\mathcal{A}_l - N\mathcal{D}_0)]$$

which can determine all eigenvalues of the matrix T_k since these eigenvalues are composed of N-multiple eigenvalues of the matrix S_k. The remaining problem is how to evaluate the eigenvalues matrix S_k. Generally, it is very difficult to give exact expressions of these eigenvalues for function f of the general form. Therefore it is also difficult to derive expressions of the corresponding Lyapunov exponents. Here we take a rough estimation. According to formula (21) for Lyapunov exponents, to make one Lyapunov exponent of the coupled systems positive, we chose such a coupling form and strength that the matrix $I+\delta t(\mathcal{A}_k-N\mathcal{D}_0)$ has one eigenvalue whose norm is more than 1 for all k. In this case, then one easily sees that the coupled systems have one positive Lyapunov exponent even though all Lyapunov exponents of the uncoupled system are currently zero or negative.

For clarity, consider the famous Lorenz system and a system of the coupled Lorenz systems. We will numerically show that the excitation effect of coupling is also conspicuous in the case of the chaotic attractor.

The uncoupled Lorenz system is

$$\begin{cases}\dfrac{dx_1}{dt} = a(x_2 - x_1)\\[2mm] \dfrac{dx_2}{dt} = cx_1 - x_1x_3 - x_2\\[2mm] \dfrac{dx_3}{dt} = x_1x_2 - bx_3\end{cases} \tag{23}$$

and the coupled Lorenz systems are assumed as

$$\begin{cases}\dfrac{dX}{dt} = f(X) + (y_1 - x_1)\overline{D}\\[2mm] \dfrac{dY}{dt} = f(Y) + (x_1 - y_1)\overline{D},\end{cases} \tag{24}$$

where $X=(x_1,x_2,x_3)$, $Y=(y_1,y_2,y_3)$, $f(X)=(a(x_2-x_1),cx_1-x_1x_3-x_2,x_1x_2-bx_3)$, and $\overline{D}=d(1,0,0)$ with $d>0$. Equation (24) may be considered a special case of Eq. (2) since $\mathcal{D}_1=-\overline{D}$ and $\mathcal{D}_2=\overline{D}$ in notations corresponding to Eq. (2).

Similar to the analysis in Sec. II, besides three characteristic values of the Jacobian matrix of the uncoupled Lorenz system at the steady state, the Jacobian matrix $\mathcal{B}$ of the

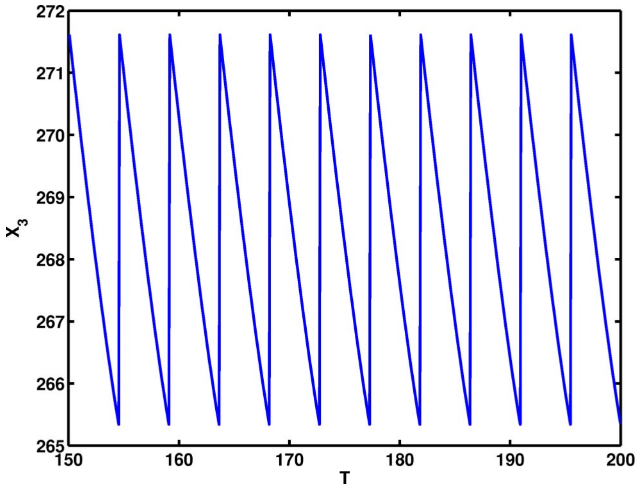

FIG. 5. Time evolution of the third component (x_3) of the periodic orbit of the uncoupled Lorenz system with parameter values $a=10$, $b=\frac{8}{3}$, and $c=23.85$. The initial values are (0, 10.74, −8.76)

coupled Lorenz systems (24) has another three characteristic values determined by the following polynomial:

$$\lambda^3 + (a+b+1+2d)\lambda^2 + [b(a+c) + 2(b+1)d]\lambda + 2ab(c-1) + 2bcd = 0. \tag{25}$$

The uncoupled Lorenz system produces a Hopf bifurcation when $(a+b+1)(a+c)=2a(c-1)$ with a set of the parameters $a=10$, $b=\frac{8}{3}$, and $c=\frac{470}{19}\simeq 24.73$. Now, we set $c=23.85$. The corresponding periodic solution of the uncoupled Lorenz system is shown in Fig. 5. For fixed $c=23.85$, to make the coupled Lorenz systems (24) chaotic, it is necessarily required that the solution of Eq. (25) is a pair of complex conjugates with positive real parts (a similar requirement is found to hold for the classical Lorenz attractor). This case implies that the equilibrium point of the coupled Lorenz systems is a saddle focus. Therefore we impose the condition

$$\Delta > 0,\ F(d) \equiv \sqrt[3]{-\frac{q}{2}+\sqrt{\Delta}} + \sqrt[3]{-\frac{q}{2}-\sqrt{\Delta}} - \frac{2p_1}{3} < 0, \tag{26}$$

where $\Delta = \frac{1}{4}p_3^2 - \frac{1}{108}p_1^2p_2^2 + \frac{1}{27}p_1^3p_3 - \frac{1}{6}p_1p_2p_3 + \frac{1}{27}p_2^3$ with $p_1=a+b+1+2d$, $p_2=b(a+c)+2(b+1)d$, $p_3=2ab(c-1)+2bcd$, $q=p_3-p_1p_2/3+2p_1^2/27$. For algebraical inequalities (26), we can obtain a conservative estimation: $6.5<d<12.5$ at fixed $a=10$, $b=\frac{8}{3}$, and $c=23.85$, whereas the range of parameter d obtained by the numerical simulation is shown in Fig. 6.

Figure 7 shows that the coupled Lorenz systems have a chaotic attractor for $d=10$. The largest Lyapunov exponents corresponding to Figs. 5 and 7, respectively, are plotted in Fig. 8. Figures 5, 7, and 8 clearly indicate that although the uncoupled Lorenz system is in the limit cycle (Fig. 5), its potential chaotic attractor (Fig. 7) is excited due to the effect of the coupling.

Similar to the case of the limit cycle, here we especially emphasize that coupling can excite or recover the Lorenz attractor from the uncoupled Lorenz system only when the uncoupled system is in the "marginal" state to the chaotic attractor. For example, at fixed $a=10$ and $b=\frac{8}{3}$, when $23.638\leqslant c\leqslant 23.875$ (in this case, the uncoupled Lorenz system is in the marginal state to a Lorenz attractor since it is actually chaotic when $c=23.88$), there are d_{10} and d_{20} such that the coupled Lorenz systems are chaotic or chaotically synchronized for $d_{10}\leqslant d\leqslant d_{20}$. However, when $c=23.63$ (even though it is close to 23.638), there is no coupling strength such that the coupled Lorenz systems are chaotic (see Fig. 9). In fact, numerical simulation has verified that the coupled Lorenz system has dynamics of no other type except that all trajectories tend to a fixed point for all coupling strengths at fixed $a=10$, $b=\frac{8}{3}$, and $c=23.63$. This case is different from that in Ref. [41], where an increase in coupling strength can push a system to undergo a series of bifurcations.

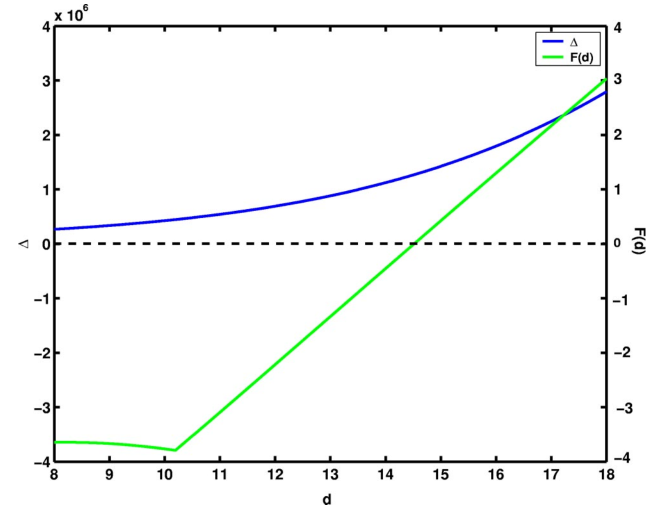

FIG. 6. The dependence relationship of Δ and $F(d)$ on parameter d.

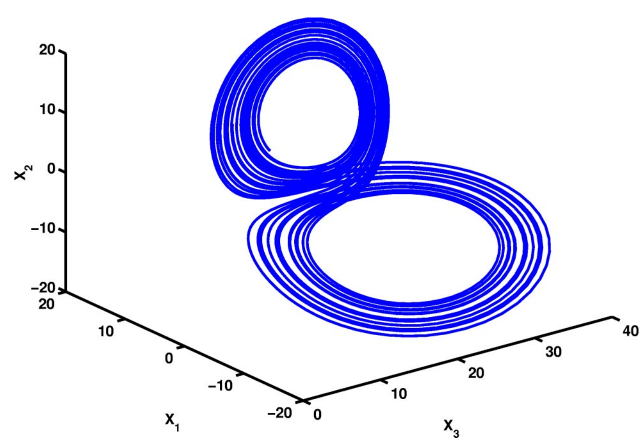

FIG. 7. Phase diagram of projection of a chaotic attractor in the coupled Lorenz systems (24) with parameters $a=10$, $b=\frac{8}{3}$, $c=23.85$, and $d=10$. The initial values are $(x_1,x_2,x_3,y_1,y_2,y_3)=(-1.5,1.8,1.5,-2.5,1.5,2.3)$. Projection of the chaotic attractor is practically an excited Lorenz attractor.

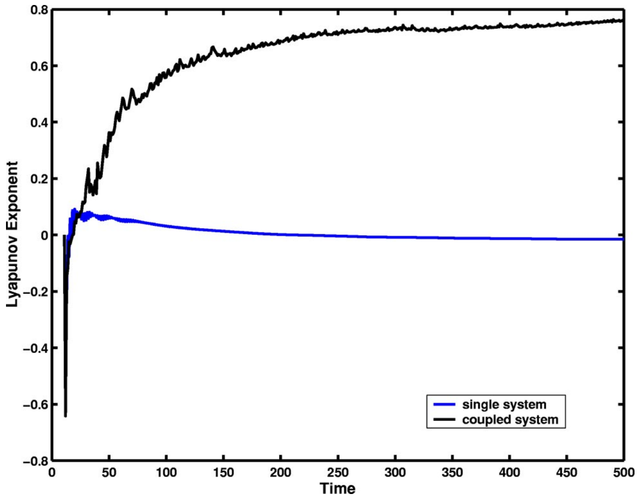

FIG. 8. Time evolution of the largest Lyapunov exponents corresponding to Figs. 5 and 7, where parameters are $a=10.0$, $b=\frac{8}{3}$, $c=23.63$, and the coupling coefficient is $d=10.0$. The largest Lyapunov exponent of the uncoupled Lorenz system with the initial condition $(-1.5, 1.8, 1.5)$ is negative and near 0.0 whereas that of the coupled Lorenz systems with the initial condition $(-1.5, 1.8, 1.5, -2.5, 1.5, 2.3)$ is positive and near 0.7606 with Lyapunov dimension 2.8816.

IV. CONCLUSION

Both theoretical analysis and numerical examples have indicated that coupling indeed has a certain excitation ability to excite or recover some dynamics of the uncoupled system. We have shown by examples that there is a threshold of coupling strength: when the coupling strength goes beyond this threshold, a limit cycle or chaotic attractor of the uncoupled system will be excited or recovered in the above-mentioned sense. Moreover, phase synchronization can occur.

Similar to the effect of noise, coupling acts as a compensating energy to "lift" dynamics of the uncoupled system and to push the coupled systems to reach synchronization even though coupling coefficients satisfy the conservation condition (i.e., the total energy of the coupled systems keeps invariant). Therefore such a synchronization due to excitation effects of coupling may be considered a self-organization process. However, it is different from stochastic resonance or coherence resonance in Refs. [5–7], where the cooperative behavior is chiefly due to effects of noise, and also different from the classical synchronization where coupling mainly synchronizes the original dynamics of the uncoupled system.

These interesting excitation functions of coupling are of significance not only in theory on dynamics of nonlinear dynamical systems but also in biological applications. In particular, such excitation functions of coupling might make living organisms harmoniously organize their various apparatuses and actively accomplish mutual communications among cells.

Finally, we point out that although coupling has excitation functions in the case of chaotic attractors, we have not given any rigorous theoretical result, and more study is required.

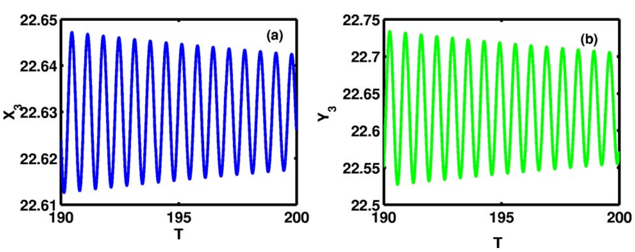

FIG. 9. An example showing that coupling cannot excite the original potential Lorenz attractor in the uncoupled Lorenz system when the uncoupled Lorenz system is not in the marginal state to the chaotic attractor, where parameters are $a=10.0$, $b=\frac{8}{3}$, $c=23.63$, and coupling coefficients are $d=10.0$. (a) Time evolution of the third component x_3 of the uncoupled Lorenz system with the initial condition $(-1.5, 1.8, 1.5)$; (b) time evolution of the third component y_3 of the coupled Lorenz systems with the initial condition $(-1.5, 1.8, 1.5, -2.5, 1.5, 2.3)$. In either case, the amplitude of the third component gradually decreases with time.

ACKNOWLEDGMENTS

The first author thanks the hospitality of the Kanazawa University of Japan, where he conducted part of this research with financial assistance from the Japanese Society for the Promotion of Science. This paper was partly supported by Special Fund for National Excellent Ph.D. Thesis.

APPENDIX A: SIMILAR MATRIX

Equation (2) may be rewritten as

$$\frac{dX}{dt} = \mathcal{F}(X) + \sum_{k=1}^{N} \mathcal{D}_k \mathcal{J}^{k-1} X, \tag{A1}$$

where

$$\mathcal{J} = \begin{pmatrix} 0 & I & 0 & \cdots & 0 \\ 0 & 0 & I & \cdots & 0 \\ \vdots & \vdots & \vdots & & \vdots \\ I & 0 & 0 & \cdots & 0 \end{pmatrix}$$

with I being a unit matrix of order m.

Denote by $\mathcal{A}$ and $\mathcal{B}$ the Jacobian matrices of Eqs. (1) and (2) evaluated at their steady states, respectively. Let $\omega_j = e^{2\pi i(j-1)/N}$ (where $1 \leqslant j \leqslant N$ and $i=\sqrt{-1}$) be N unit roots of the algebraic equation $\lambda^N - 1 = 0$ which is practically the characteristic polynomial of the matrix J, and denote by $\mathcal{P}$ the Vandermonde matrix

$$\begin{pmatrix} I & I & \cdots & I \\ \omega_1 I & \omega_2 I & \cdots & \omega_N I \\ \vdots & \vdots & & \vdots \\ \omega_1^{N-1} I & \omega_2^{N-1} I & \cdots & \omega_N^{N-1} I \end{pmatrix}.$$

Then, it is easy to verify

$$\mathcal{P}^{-1}\mathcal{B}\mathcal{P} = \mathrm{diag}(d(\omega_1 I), d(\omega_2 I), \ldots, d(\omega_N I)), \tag{A2}$$

where $d(x) = \mathcal{A} + \sum_{j=1}^{N} \mathcal{D}_j x^{j-1}$. In addition, since $d(\omega_1) = d(1) = \mathcal{A}$ from the conservation condition of coupling, the matrix

$\mathcal{B}$ can be similar to a real block matrix, that is, there exists a reversible real matrix $\mathcal{Q}$ such that

$$\mathcal{Q}^{-1}\mathcal{B}\mathcal{Q} = \begin{pmatrix} \mathcal{A} & \mathcal{O} \\ \mathcal{O} & \mathcal{R} \end{pmatrix}, \tag{A3}$$

where $\mathcal{R}$ is a certain real matrix. For clarity, we distinguish two cases.

Case $N=2K+1$. Define two $m\times m$ matrix functions:

$$\mathcal{D}_R(\vartheta) = \mathcal{D}_1 + \mathcal{A} + \mathcal{D}_2 \cos\vartheta + \mathcal{D}_3 \cos 2\vartheta + \cdots + \mathcal{D}_N \cos(N-1)\vartheta,$$

$$\mathcal{D}_I(\vartheta) = \mathcal{D}_2 \sin\vartheta + \mathcal{D}_3 \sin 2\vartheta + \cdots + \mathcal{D}_N \sin(N-1)\vartheta \tag{A4}$$

and two $Nm\times m$ matrix functions:

$$\mathcal{P}_R(\vartheta) = (I, I\cos\vartheta, I\cos 2\vartheta, \ldots, I\cos(N-1)\vartheta)^t,$$

$$\mathcal{P}_I(\vartheta) = (\mathcal{O}, I\sin\vartheta, I\sin 2\vartheta, \ldots, I\sin(N-1)\vartheta)^t, \tag{A5}$$

where t means transpose. Now, it is easy to give expressions of $\mathcal{Q}$ and $\mathcal{R}$ as follows:

$$\mathcal{R} = \mathrm{diag}\left(\begin{pmatrix} \mathcal{D}_R(\vartheta_1) & -\mathcal{D}_I(\vartheta_1) \\ \mathcal{D}_I(\vartheta_1) & \mathcal{D}_R(\vartheta_1) \end{pmatrix}, \ldots, \begin{pmatrix} \mathcal{D}_R(\vartheta_K) & -\mathcal{D}_I(\vartheta_K) \\ \mathcal{D}_I(\vartheta_K) & \mathcal{D}_R(\vartheta_K) \end{pmatrix}\right) \tag{A6}$$

and

$$\mathcal{Q} = (\mathcal{P}_R(0); \mathcal{P}_R(\vartheta_1), \mathcal{P}_I(\vartheta_1); \ldots; \mathcal{P}_R(\vartheta_K), \mathcal{P}_I(\vartheta_K)),$$

where $\vartheta_j = 2\pi j/(2K+1)$ for $1\leqslant j\leqslant K$.

Case $N=2K$. Similarly,

$$\mathcal{R} = \mathrm{diag}\left(\mathcal{D}_R(\pi); \begin{pmatrix} \mathcal{D}_R(\vartheta_1) & -\mathcal{D}_I(\vartheta_1) \\ \mathcal{D}_I(\vartheta_1) & \mathcal{D}_R(\vartheta_1) \end{pmatrix}; \ldots; \begin{pmatrix} \mathcal{D}_R(\vartheta_{K-1}) & -\mathcal{D}_I(\vartheta_{K-1}) \\ \mathcal{D}_I(\vartheta_{K-1}) & \mathcal{D}_R(\vartheta_{K-1}) \end{pmatrix}\right) \tag{A7}$$

and

$$\mathcal{Q} = (\mathcal{P}_R(0), \mathcal{P}_R(\pi); \mathcal{P}_R(\vartheta_1), \mathcal{P}_I(\vartheta_1); \ldots; \mathcal{P}_R(\vartheta_K), \mathcal{P}_I(\vartheta_K)),$$

where $\vartheta_j = 2\pi j/(2K)$ for $1\leqslant j\leqslant K-1$, $\mathcal{D}_R(\pi) = \mathcal{A} + \Sigma_{i=1}^{N}(-1)^{i+1}\mathcal{D}_i$, $\mathcal{P}_R(0) = (I, I, \ldots, I)^t$, and $\mathcal{P}_R(\pi) = (I, -I, I, \ldots, I, -I)^t$.

APPENDIX B: CONDITIONS FOR LIMIT CYCLE OF COUPLED BRUSSELATORS

Consider coupled N identical Brusselators with the form (2). We show that the coupled Brusselators have a limit cycle even though the uncoupled Brusselator is still in the stable state but not far away from a limit cycle.

For simplicity, consider the case of $N=2K$, where K is a positive integer. We then have $\mathcal{D}_R(\pi) = \mathcal{A} + \Sigma_{j=1}^{N}(-1)^{j-1}\mathcal{D}_j$. Assume $\mathcal{D}_j = \mathrm{diag}(d_j^{(1)}, d_j^{(2)})$ with $d_j^{(1)}>0$ and $d_j^{(2)}>0$ $(1\leqslant j\leqslant N)$. Note that the characteristic polynomial of $\mathcal{D}_R(\pi)$ is

$$\lambda^2 + \xi\lambda + \eta = 0, \tag{B1}$$

where

$$\xi = a^2 - 1 + \mu\sum_{j=1}^{N}(-1)^j(d_j^{(2)} + d_j^{(2)}),$$

$$\eta = a^2 + a^2\sum_{j=1}^{N}(-1)^j d_j^{(1)} + (1-\mu)\sum_{j=1}^{N}(-1)^j d_j^{(2)} + \left(\sum_{j=1}^{N}(-1)^j d_j^{(2)}\right)\left(\sum_{j=1}^{N}(-1)^j d_j^{(2)}\right).$$

When $\eta<0$, Eq. (B1) has one positive root. Also, note that

$$\sum_{j=1}^{N}(-1)^j d_j^{(l)} = \sum_{j=2}^{N}[1+(-1)^j]d_j^{(l)} > 0, \ l=1,2.$$

Thus $\eta<0$ implies

$$\mu > 1 + \frac{a^2\sum_{j=2}^{N}[1+(-1)^j]d_j^{(1)}}{\sum_{j=2}^{N}[1+(-1)^j]d_j^{(2)}} + \sum_{j=2}^{N}[1+(-1)^j]d_j^{(1)}. \tag{B2}$$

However, $\mu\leqslant a^2+1$. Therefore

$$a^2\sum_{j=2}^{N}[1+(-1)^j](d_j^{(2)} - d_j^{(1)}) > \left\{\sum_{j=2}^{N}[1+(-1)^j]d_j^{(1)}\right\}\cdot\left\{\sum_{j=2}^{N}[1+(-1)^j]d_j^{(2)}\right\}. \tag{B3}$$

Finally, when Eq. (B2) together with $\mu\leqslant a^2+1$ and Eq. (B3) are satisfied, the coupled Brusselators have a stable limit cycle even though the uncoupled Brusselator is currently in the stable steady state.

[1] V. S. Anishchenko, T. E. Vadivasova, D. E. Postnov, and M. A. Safonova, Int. J. Bifurcation Chaos Appl. Sci. Eng. **2**, 633 (1992).
[2] M. Rosenblum, A. S. Pikovsky, and J. Kurths, Phys. Rev. Lett. **76**, 1804 (1996).
[3] A. S. Pikovsky, M. G. Rosenblum, G. V. Osipov, and J. Kurths, Physica D **104D**, 219 (1997).
[4] T. S. Zhou, J. H. Lv, G. Chen, and Y. Tang, Phys. Lett. A **301**, 231 (2002).
[5] A. S. Pikovsky, M. G. Rosenblum, and J. Kurths, *Synchronization: A Universal Concept in Nonlinear Sciences* (Cambridge University Press, Cambridge, England, 2001).
[6] V. Anishchenko, F. Moss, A. Neiman, and L. Schimansky, Phys. Usp. **42**, 7 (1999).
[7] K. Wiessenfeld and F. Moss, Nature (London) **373**, 33 (1995).
[8] D. Sigeti and W. Horsthemke, J. Stat. Phys. **54**, 1217 (1989).
[9] A. S. Pikovsky and J. Kurths, Phys. Rev. Lett. **78**, 775 (1997).
[10] S. K. Han, T. G. Yim, D. E. Postnov, and O. V. Sosnovtseva, Phys. Rev. Lett. **83**, 1771 (1999).
[11] H. Gang, T. Ditzinger, C. Z. Ning, and H. Haken, Phys. Rev. Lett. **71**, 807 (1993).
[12] J. J. Tyson, Ann. N.Y. Acad. Sci. **316**, 279 (1979).
[13] E. N. Best, Biophys. J. **27**, 87 (1979).
[14] V. Torre, Biol. Cybern. **17**, 137 (1975).
[15] J. Bélar and P. Holmes, Q. Appl. Math. **32**, 193 (1984).
[16] T. Shinbrot, C. Grebogi, E. Ott, and J. A. York, Nature (London) **363**, 411 (1993).
[17] D. McMillen, N. Kopell, J. Hasty, and J. J. Collins, Proc. Natl. Acad. Sci. U.S.A. **99**, 679 (2002).
[18] V. I. Krinsky and A. V. Kholopov, Biofizika **12**, 524 (1967).
[19] R. Fitz-Hugh, Biophys. J. **1**, 445 (1961).
[20] G. J. Rozansky, J. Jalife, and G. K. Moe, Circulation, **69**, 163 (1984).
[21] A. T. Winfree, *The Geometry of Biological Time* (Springer, Berlin, 1980).
[22] E. C. Zeeman, in *Dynamical Systems*, edited by M. M. Peixoto (Academic Press, New York, 1973), pp. 683–741.
[23] R. E. Mirollo and S. H. Strogatz, SIAM J. Appl. Math. **6**, 1645 (1990).
[24] M. E. Taga and B. L. Bassler, Proc. Natl. Acad. Sci. U.S.A. **100**, 14549 (2003).
[25] B. Perbal, Cell Commun. Signaling **1**, 1 (2003).
[26] D. E. Postnov, O. V. Sosnovtseva, S. K. Han, and T. G. Yim, Int. J. Bifurcation Chaos Appl. Sci. Eng. **10**, 2541 (2000).
[27] I. Z. Kiss, Y. Zhai, J. L. Hudson, C. Zhou, and J. Kurths, Chaos **13**, 267 (2003).
[28] M. Zhan, G. W. Wei, C. H. Lai, Y. C. Lai, and Z. Liu, Phys. Rev. E **66**, 036201 (2002).
[29] G. Balazsi, A. Cornell-Bell, A. B. Neiman, and F. Moss, Phys. Rev. E **64**, 041912 (2001).
[30] G. Balazsi, A. Cornell-Bell, and F. Moss, Chaos **13**, 515 (2003).
[31] T. S. Zhou and S. C. Zhang, Physica D **151**, 199 (2001).
[32] J. H. Lv, T. S. Zhou, and S. C. Zhang, Chaos, Solitons Fractals **14**, 529 (2002).
[33] P. Davis, *Circular Matrices* (Wiley, New York, 1979).
[34] J. C. Alexander and G. Auchmuty, Arch. Ration. Mech. Anal. **93**, 253 (1986).
[35] T. S. Zhou, L. N. Chen, R. Q. Wang, and K. Aihara, Genome Informatics **15**, 223 (2004).
[36] T. S. Zhou, L. J. Yang, and Y. Tang (unpublished).
[37] C. C. Chow, Physica D **118**, 343 (1998).
[38] G. Nicolis and I. Prigogine, *Self-organization in Nonequilibrium Systems* (Wiley Interscience, New York, 1977).
[39] C. F. Zhang, *Theory of Differential Equations* (Beijing Scientific Press House, 1985).
[40] H. Tong, *Non-linear Time Series: A Dynamical System Approach* (Oxford University Press, New York, 1990).
[41] S. Bahar, Fluct. Noise Lett. **4**, L87 (2004).